

A photodefinable thermally-responsive hydrogel bilayer with SU-8

Paul Chong¹, Grace Woods²

SNF Mentor: Swaroop Kommera

Industry Mentors: Mark Zdeblick, Tony Ricco

¹ Department of Chemistry, Stanford University

² Department of Applied Physics, Stanford University

Table of Contents

[Motivation](#)

[Stimuli-Responsive Hydrogel](#)

[Properties of SU-8](#)

[Hydrogel/SU-8 Interface](#)

[Methods](#)

[5.1 Oxygen plasma](#)

[5.2 Chemical functionalization](#)

[5.3 Assessment of Hydrogel layer](#)

[Future Work](#)

[Acknowledgements](#)

[References](#)

1. Motivation

Visual processing begins in the retina with retinal ganglion cells (RGCs), the output neurons in the eye.¹ 30 different subtypes of RGCs are distributed across the retina with varying densities in their mosaic arrangements.²⁻⁴ While electrophysiology remains the gold standard for evaluating the functional viability of neurons, existing probes for neural recording suffer from several limitations that make them incompatible with recording from the retina *in vivo*. Commonly used multi-electrode arrays (MEAs) are rigid and flat, thus unable to interface seamlessly with the highly curved surface of the retina. We aim to address these limitations by utilizing a flexible and injectable open mesh probe design (**Fig. 1a**) in conjunction with a thermally responsive hydrogel coating facilitating shape change into a hemispherical array to conformally coat the retina upon intravitreal injection. Expanding on this study, we anticipate that our thermally responsive retinal probe will conformally coat the entire retina with a flexible, 64-channel MEA in a macroporous mesh platform, which transmits 95% of visible light and preserves the natural functions of the eye.⁵

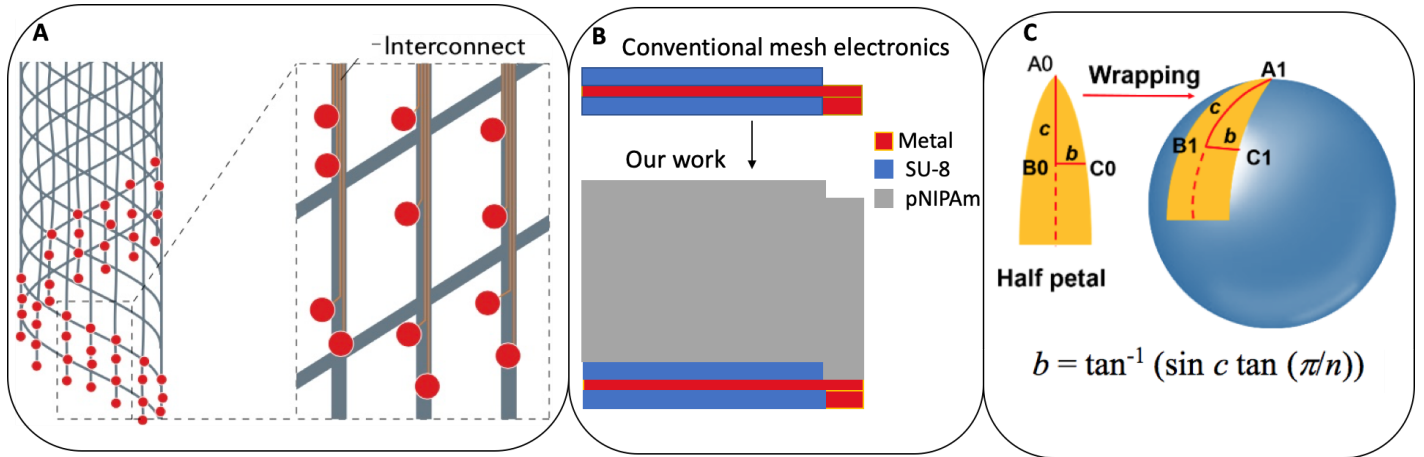


Fig. 1 Motivation for thermally-responsive mesh electronics. (A) Schematic of demonstrating ultrathin, flexible mesh electronics.⁶ (B) Cross-section of conventional double-sided mesh electronics and our work, where we pattern a thick layer of pNIPAM on top of the insulating SU-8 structure. The pNIPAM layer is approximately an order of magnitude greater than that of conventional mesh electronics. (C) When our final device is injected into the vitreous space of the eye, its petal-like structure will form a hemispherical interface with the retinal surface.⁷

The principle of our device is as follows: a relatively thick layer ($\sim O(10\text{'s } \mu\text{m})$) of thermally-responsive hydrogel patterned on top of ultrathin mesh electronics ($\sim O(\mu\text{m})$) (**Fig. 1b**) will result in 2D to 3D hemispherical actuation when subjected to body temperature within the eye (**Fig. 1c**). The value of this project to SNF is realized through the expansion of the diversity of materials that may be used by future users of SNF, as well as the development and optimization of a polymer-hydrogel bilayer.

2. Stimuli-Responsive Hydrogel

Stimuli-responsive materials have found significant application in functional devices for their conversion of energy forms, from magnetothermal materials such as iron oxide for enhanced actuation in microgrippers⁸ to stimulation of neurons through mechanoluminescent nanoparticles⁹. Our project focuses on a hydrogel whose properties change with the application or reduction of thermal energy.¹⁰ In particular, above its lower critical solution temperature (LCST), poly(*N*-isopropylacrylamide) (pNIPAm) hydrogel releases water and deswells leading to an anisotropic reduction in volume.¹¹ This property has been leveraged in a multitude of biomedical applications, such as stimuli-responsive microgrippers, controlled release of small molecules, and microgel films for cell culture.^{8,12,13}

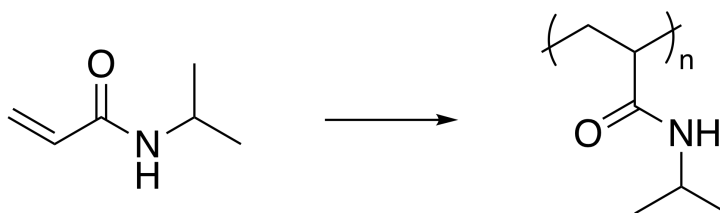


Figure 2. *N*-isopropylacrylamide (NIPAm) monomer polymerizes to form linear poly(*N*-isopropylacrylamide) polymer.

NIPAm may be copolymerized with other monomers in order to tune the LCST and other chemical and mechanical properties.¹⁴ Poly(*N*-isopropylacrylamide-*co*-acrylic acid) (pNIPAm-AAc), a well-studied copolymer of pNIPAm, was chosen for this study. In this hydrogel copolymer, the introduction of acrylic acid tunes sensitivity to heat, pH, and ionic strength.¹⁵

In order to make this material compatible with optical lithographic techniques, we developed an array of pNIPAm/NIPAm photoresists with different formulations. In particular, there was a wide range of freedom in optimizing our photoresist, from the types and amounts of solvents used to the concentration of photoinitiator and whether to include polymerized NIPAm for mechanical reinforcement (**Table 1**).

Table 1.

Solvent	Viscosity (Pa·s)	Comments
Ethylene glycol	1.61×10^{-2}	Resist too thin to spincoat
Propylene glycol	0.042	Resist performs better than ethylene glycol, but still lacks structure to withstand spincoating

Glycerol	1.412	Resist thickness on par with standard negative photoresist (ref. SU-8 3005)
Propylene glycol + Glycerol (1:1) ¹	~ 0.7	Viscosity is improved
1-butanol	2.573×10^{-3}	Resist is thin, but appears to adhere well; Integrating pNIPAm into resist formulation greatly improves processing

3. Properties of SU-8

SU-8 is an epoxy-based negative photoresist that is a standard for high aspect ratio structures in photolithography and has found significant applications in microfluidics and as an insulating material for implantable devices. The monomer of SU-8 consists of a multifunctional macromonomer with an average of eight epoxy groups per unit available for reaction (**Fig. 3**). Upon exposure to UV light, a triarylsulfonium/hexafluoroantimonate salt acts as a photoacid generator and epoxy groups become protonated, which initiates ring-opening polymerization to form a highly crosslinked network structure.

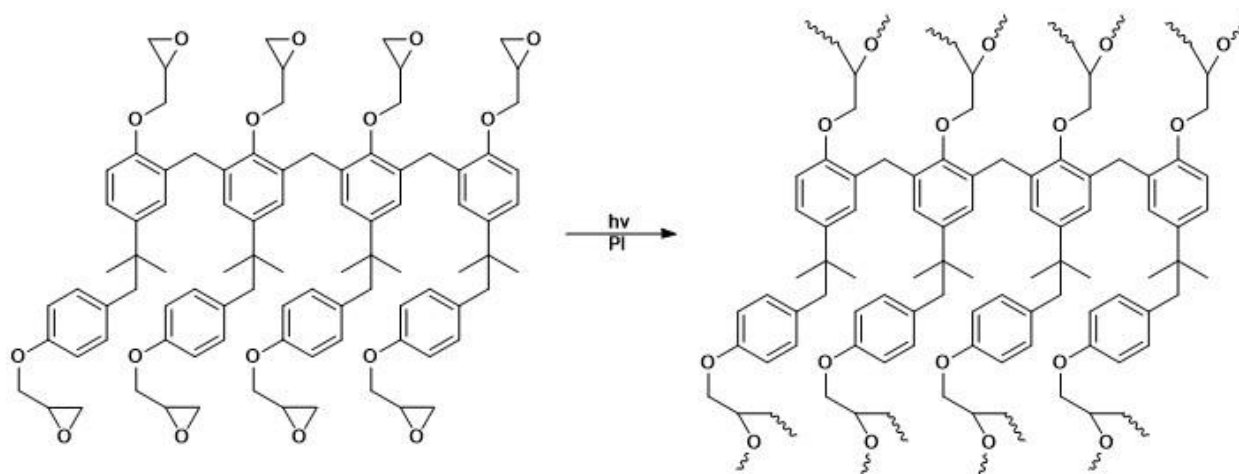


Figure 3. Photocrosslinking of SU-8 monomer to form the cured network polymer.

¹ We tested other ratios of propylene glycol:glycerol throughout this quarter and found that formulations with greater glycerol content than 2:1 propylene glycol:glycerol were too viscous and we ran into difficulty with its solubility limit.

4. Hydrogel/SU-8 Interface

Insulating layers for implantable electronic devices are typically hydrophobic materials which act as barriers against water diffusion. With this difference in hydrophilicity, along with the large difference in mechanical properties, it follows that a hydrogel would have poor adhesion to organic polymer-based insulating materials without any surface treatment. Some strategies that have been employed to improve wetting and adhesion to SU-8 films include oxygen plasma treatment and chemical surface modification.^{16,17}

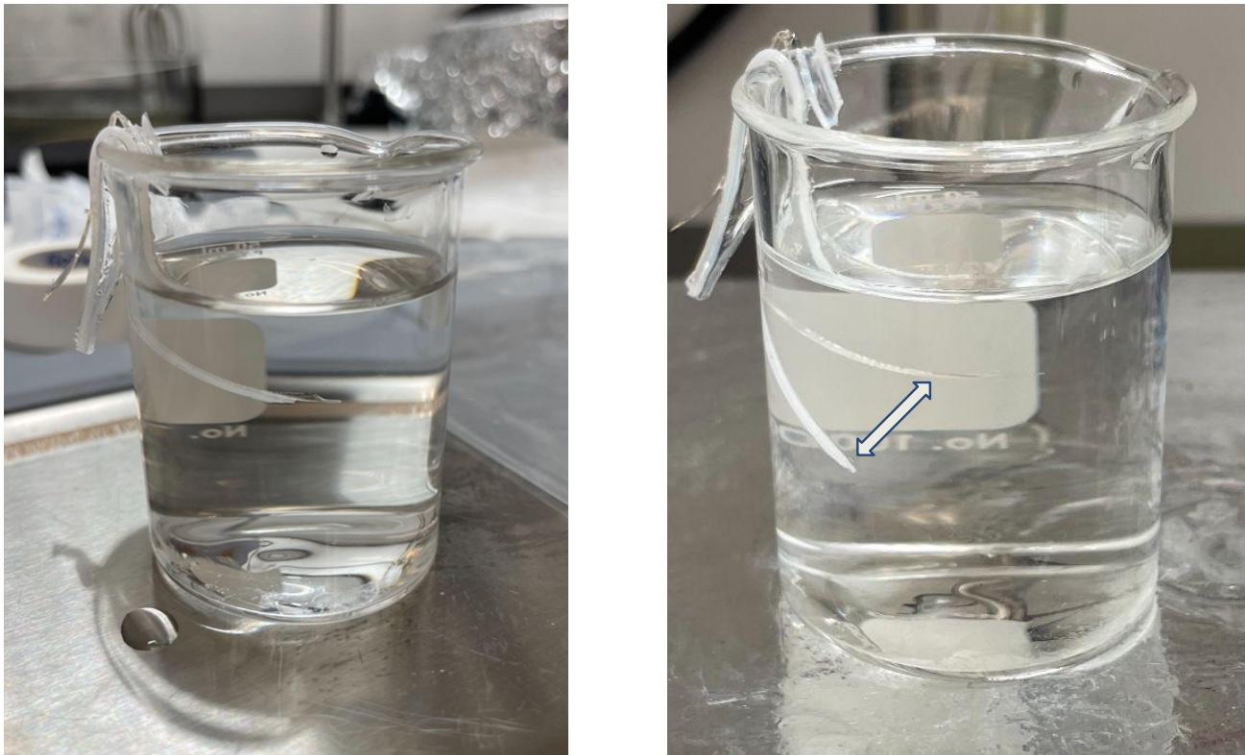


Figure 4. Demonstration of poor adhesion between crosslinked SU-8 and pNIPAm hydrogel bilayers. Upon submersion into an aqueous solution, SU-8 and pNIPAm layers delaminate.

5. Methods

A bilayer of SU-8 and pNIPAm-AAc hydrogel were patterned onto bare Silicon substrates (3" Si wafers) and glass substrates (1 mm thick Fisher microscope slides). Our choice of substrate was flexible due to the fact that SU-8, once crosslinked, adheres well to most substrates and our decision was ultimately to limit the use of available funding.

The patterning of SU-8 was conducted by spincoating the substrate with SU-8 3005 at 1000 rpm to achieve a film with an approximate thickness of 10 μm . The pre-exposure bake was then

conducted at 65 °C for 1 min and 95 °C for 1 min on a programmable hotplate. The photopatterning of SU-8 was conducted with the Karlsuss mask aligner (i-line, 15 mW/cm²) for 8.5 seconds. The SU-8 was then baked at 65 °C for 1 min and 95 °C for 1 min to complete the crosslinking and then developed in SU-8 developer for 2 min, followed by an IPA bath and rinse, and finished with blow drying. Details for improving the adhesion between the cured SU-8 and hydrogel are described in sections below.

For the hydrogel-based photoresist formulation, pNIPAm (0.4 g), NIPAm (3 g), *N,N'*-methylenebis(acrylamide) (180 mg), and acrylic acid (0.3 mL) were fully dissolved in 1-butanol (7.5 mL) by stirring in a 20-mL scintillation vial with stir bar at room temperature overnight. The scintillation vial was then covered with aluminum foil and lithium phenyl(2,4,6-trimethylbenzoyl)phosphinate (30 mg) was added and stirred until dissolved. In the formulation, pNIPAm, NIPAm, and acrylic acid monomers form the base of the resist and *N,N'*-methylenebis(acrylamide) acts as a crosslinker to create the hydrogel 3D network polymer. Lithium phenyl(2,4,6-trimethylbenzoyl)phosphinate is a water-soluble type I radical photoinitiator with a broad spectrum of activation wavelengths. Our pNIPAm-AAc photoresist has been processed in two key schemes: (1) dropcasting and (2) spincoating, depending on the formulation of the resist. As described in Section 2, there was significant freedom in formulating our resist, whose composition affected its propensity to form a thin film under spinning conditions. Ultimately, we found that we achieve the best results, in both photopatternability and actuation, by dropcasting our resist onto the SU-8 structures and the substrate.

The pNIPAm-AAc coated substrate was then loaded into the Karlsuss mask aligner for exposure. For methods of flood exposure, the substrate was loaded into the machine without a photomask or a blank photomask and sections of exposure were defined by placing a custom pattern of aluminum foil to block the incident UV light. For methods of photopatterning structures, a photomask that was designed using AutoCAD and patterned with the Heidelberg direct write machine (Resist: AZ1518, Dose: 90 mJ/cm², Defocus: -2, Developer: AZ 1:1 for 1 min, Chrome Etchant: Ceric ammonium nitrate) was loaded into the Karlsuss. In order to prevent the crosslinked hydrogel layer from attaching to the mask during contact, either through the initial contact through wedge error correction (WEC) or during exposure to optimize precision of structures, we add glass substrates symmetrically along the edges of the substrate as a spacer. An unfortunate consequence of this is that the resolution of structures will then be limited by the alignment and diffraction of the UV source from the transparent-opaque boundaries on the photomask. This can easily be ramified, however, by transitioning this protocol into a direct write system, such as the Heidelberg.

5.1 Oxygen plasma

Oxygen plasma treatment is utilized for removal of organic scum, etching structures, and modification of surfaces for improved hydrophilicity. Therefore, the hydrophobic surface

structure and composition of cured SU-8 naturally lends itself to oxygen plasma treatment. In particular, x-ray photoelectron spectroscopy (XPS) measurements conducted on cured SU-8 and plasma-treated SU-8 have demonstrated that the surface composition of untreated SU-8 dramatically transitions after plasma treatment. Untreated SU-8 predominantly contains carbon (84.5%), containing aromatic carbon (C-C) and ether carbon (C-O), and oxygen (15.3%), while plasma-treated SU-8 surfaces shift to a 66.3% composition of carbon and a 30.2% composition of oxygen. This is hypothesized to be due to the recruitment of carboxylic acids and aldehyde groups generated through partial oxidation, as well as a reduction of aromatic carbon groups.¹⁶

Oxygen plasma treatment was conducted on cured SU-8 structures using the March Instruments PX-250 Plasma Asher in the SNSF Flexible Cleanroom with an oxygen flow of 3 sccm at 100 W for 120 seconds in direct mode. Samples were first transferred to our laboratory to confirm enhanced wettability (**Fig. 5a**) future samples were then transferred back to SNF for further processing.

While plasma-treated SU-8 encouraged better adhesion between uncured pNIPAm-AAc during spincoating and dropcasting, the subsequent development stage post-UV exposure removed all exposed structures, indicating poor adhesion between the SU-8 and the pNIPAm-AAc (**Fig. 5b**).

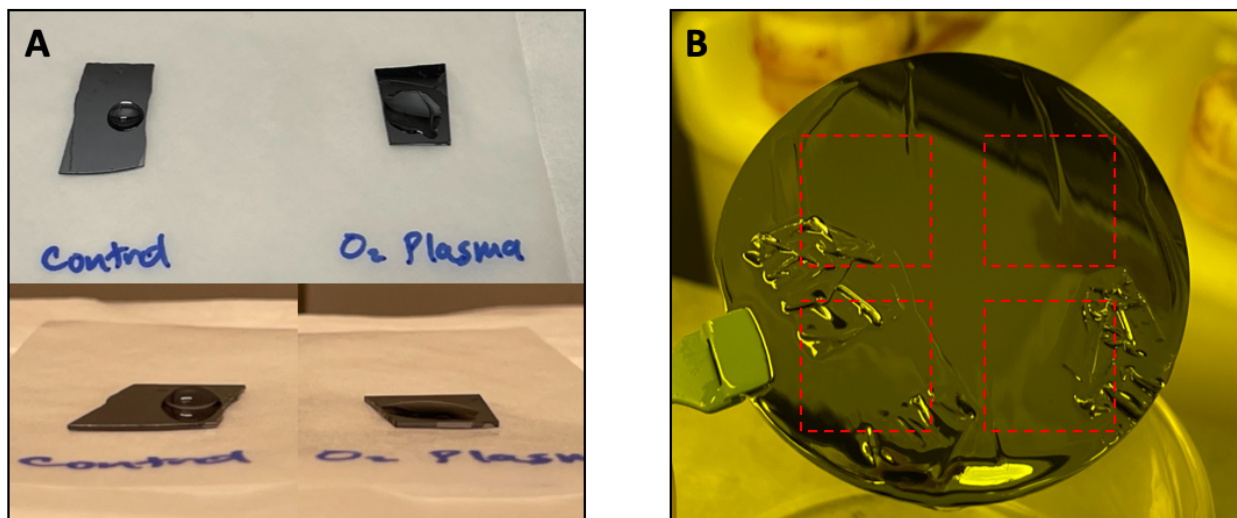


Figure 5. Oxygen-plasma treated SU-8. (A) Wettability of plasma-treated cured SU-8 on silicon substrates is greatly improved by inspection of the surface tension of a droplet of MilliQ water. (B) Gentle development removes square structures of exposed pNIPAm-AAc. The red-dashed square overlays indicate the intended pattern.

5.2 Chemical functionalization

In this work, two approaches were taken to chemically modify SU-8 to improve adhesion to pNIPAm-AAc. In the first approach, 2-hydroxyethyl acrylate (**Fig. 6**) was mixed into the SU-8

photoresist before deposition and patterning. Although adhesion improved, the bilayer with pNIPAm-AAc eventually delaminated in water with the swelling of the hydrogel layer. In the second approach, cured SU-8 was immersed in pure Jeffamine D-230, a common liquid epoxy curing agent, for 5 minutes, followed by 365-nm UV exposure (3 W, 5 min). The SU-8 layer was then air-dried and the pNIPAm-AAc resist was dropcast on top and cured. This method gave the best adhesion with pNIPAm-AAc hydrogel to form a bilayer which survived sonication, immersion in water for extended periods of time (days), and repeated deswelling and swelling cycles in water with change in temperature. The exact mechanism which promotes adhesion with the use of Jeffamine D-230 is not yet known and requires further study. We hypothesize that the primary amine groups in Jeffamine D-230 may react with epoxy groups of SU-8 as well as carboxylic acid and/or amide functional groups of pNIPAm-AAc, producing a covalently bonded pNIPAm-AAc layer on the SU-8 film.

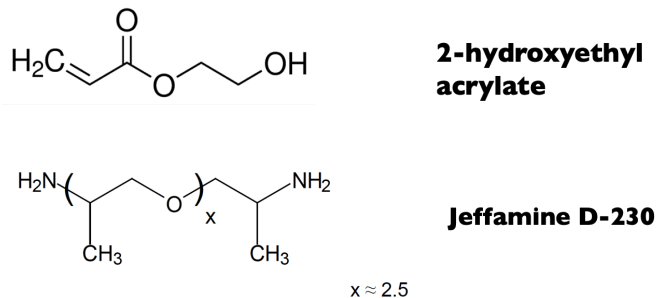


Figure 6. Structures of 2-hydroxy acrylate and Jeffamine D-230.

5.3 Assessment of Hydrogel layer

In order to assess whether the hydrogel layer survives photopatterning and development, we take advantage of its ability to swell through its recruitment of water. In particular, we submerge the photopatterned bilayer of SU-8/pNIPAm-AAc into a concentrated aqueous solution containing methylene blue, which is then taken up into the hydrogel layer for further optical imaging (**Fig. 7**).

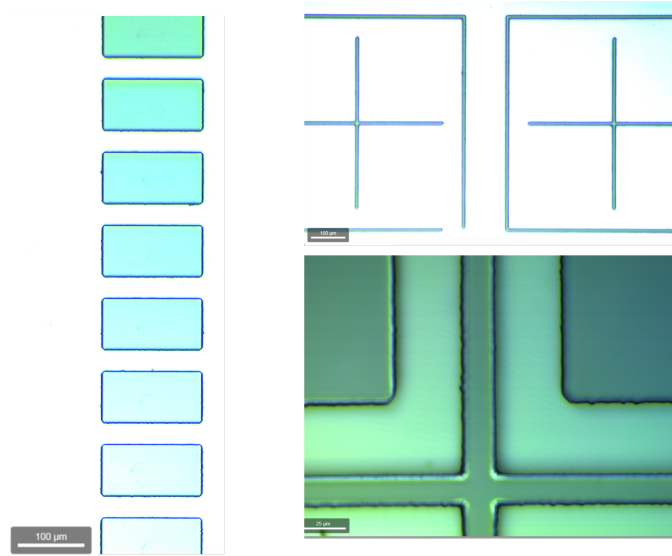


Figure 7. Photopatterned SU-8/pNIPAM-AAc rectangular beams. (Left) $200 \times 100 \mu\text{m}^2$ rectangular beams of SU-8 and methylene blue-dyed pNIPAM structures imaged with bright field optical microscopy. (Right) Alignment markers of (top) fine $1 \mu\text{m}$ structures and (bottom) $10 \mu\text{m}$ structures.

6. Future Work

We aim to continue this work with the following experiments: (1) Development of a spin speed vs. thickness curve for the pNIPAM-AAc resist to be able to control film thickness, (2) measurement of actuation amplitude for bilayer beams of varying SU-8 and pNIPAM-AAc thicknesses, (3) finite element analysis to study the actuation of bilayer beams and the final device, and (4) accelerated aging tests for testing the adhesion of SU-8 and pNIPAM-AAc in long-term implanted device.

7. Acknowledgements

We would like to extend our gratitude to our mentors, Swaroop, Mark, and Tony, for their consistent guidance and support throughout this quarter, in addition to their generous senses of humor. We would also like to thank Professors Jonathan Fan and Roger Howe for their support and encouragement for our exploratory research with the SNF facilities and staff. Finally, we'd like to thank Vijay Narasimhan for his curiosity, enthusiasm, and support with our research.

8. References

- (1) Masland, R. H. The Fundamental Plan of the Retina. *Nat. Neurosci.* **2001**, *4* (9), 877–886. <https://doi.org/10.1038/nn0901-877>.
- (2) Sanes, J. R.; Masland, R. H. The Types of Retinal Ganglion Cells: Current Status and Implications for Neuronal Classification. *Annu. Rev. Neurosci.* **2015**, *38*, 221–246. <https://doi.org/10.1146/annurev-neuro-071714-034120>.
- (3) VanderWall, K. B.; Lu, B.; Alfaro, J. S.; Allsop, A. R.; Carr, A. S.; Wang, S.; Meyer, J. S. Differential Susceptibility of Retinal Ganglion Cell Subtypes in Acute and Chronic Models of Injury and Disease. *Sci. Rep.* **2020**, *10* (1), 17359. <https://doi.org/10.1038/s41598-020-71460-6>.
- (4) Tran, N. M.; Shekhar, K.; Whitney, I. E.; Jacobi, A.; Benhar, I.; Hong, G.; Yan, W.; Adiconis, X.; Arnold, M. E.; Lee, J. M.; Levin, J. Z.; Lin, D.; Wang, C.; Lieber, C. M.; Regev, A.; He, Z.; Sanes, J. R. Single-Cell Profiles of Retinal Ganglion Cells Differing in Resilience to Injury Reveal Neuroprotective Genes. *Neuron* **2019**, *104* (6), 1039–1055.e12. <https://doi.org/10.1016/j.neuron.2019.11.006>.
- (5) Hong, G.; Fu, T.-M.; Qiao, M.; Viveros, R. D.; Yang, X.; Zhou, T.; Lee, J. M.; Park, H.-G.; Sanes, J. R.; Lieber, C. M. A Method for Single-Neuron Chronic Recording from the Retina in Awake Mice. *Science* **2018**, *360* (6396), 1447–1451. <https://doi.org/10.1126/science.aas9160>.
- (6) Hong, G.; Lieber, C. M. Author Correction: Novel Electrode Technologies for Neural Recordings. *Nat. Rev. Neurosci.* **2019**, *20* (6), 376. <https://doi.org/10.1038/s41583-019-0169-6>.
- (7) Zhuang, J.; Ju, Y. S. A Tunable Hemispherical Platform for Non-Stretching Curved Flexible Electronics and Optoelectronics. *J. Appl. Phys.* **2014**, *116* (4), 044508. <https://doi.org/10.1063/1.4891460>.
- (8) Breger, J. C.; Yoon, C.; Xiao, R.; Kwag, H. R.; Wang, M. O.; Fisher, J. P.; Nguyen, T. D.; Gracias, D. H. Self-Folding Thermo-Magnetically Responsive Soft Microgrippers. *ACS Appl. Mater. Interfaces* **2015**, *7* (5), 3398–3405. <https://doi.org/10.1021/am508621s>.
- (9) Wu, X.; Zhu, X.; Chong, P.; Liu, J.; Andre, L. N.; Ong, K. S.; Brinson, K., Jr; Mahdi, A. I.; Li, J.; Fenno, L. E.; Wang, H.; Hong, G. Sono-Optogenetics Facilitated by a Circulation-Delivered Rechargeable Light Source for Minimally Invasive Optogenetics. *Proc. Natl. Acad. Sci. U. S. A.* **2019**. <https://doi.org/10.1073/pnas.1914387116>.
- (10) Bassik, N.; Abebe, B. T.; Laffin, K. E.; Gracias, D. H. Photolithographically Patterned Smart Hydrogel Based Bilayer Actuators. *Polymer* **2010**, *51* (26), 6093–6098. <https://doi.org/10.1016/j.polymer.2010.10.035>.
- (11) Nagase, K.; Yamato, M.; Kanazawa, H.; Okano, T. Poly(N-Isopropylacrylamide)-Based Thermoresponsive Surfaces Provide New Types of Biomedical Applications. *Biomaterials* **2018**, *153*, 27–48. <https://doi.org/10.1016/j.biomaterials.2017.10.026>.
- (12) Sanzari, I.; Buratti, E.; Huang, R.; Tusan, C. G.; Dinelli, F.; Evans, N. D.; Prodromakis, T.; Bertoldo, M. Poly(N-Isopropylacrylamide) Based Thin Microgel Films for Use in Cell Culture Applications. *Sci. Rep.* **2020**, *10* (1), 6126. <https://doi.org/10.1038/s41598-020-63228-9>.
- (13) Malachowski, K.; Breger, J.; Kwag, H. R.; Wang, M. O.; Fisher, J. P.; Selaru, F. M.; Gracias, D. H. Stimuli-Responsive Theragrippers for Chemomechanical Controlled Release.

- Angew. Chem. Int. Ed Engl.* **2014**, *53* (31), 8045–8049.
<https://doi.org/10.1002/anie.201311047>.
- (14) Doberenz, F.; Zeng, K.; Willems, C.; Zhang, K.; Groth, T. Thermoresponsive Polymers and Their Biomedical Application in Tissue Engineering – a Review. *Journal of Materials Chemistry B*. 2020, pp 607–628. <https://doi.org/10.1039/c9tb02052g>.
- (15) Ahiabu, A.; Serpe, M. J. Rapidly Responding pH- and Temperature-Responsive Poly (N-Isopropylacrylamide)-Based Microgels and Assemblies. *ACS Omega* **2017**, *2* (5), 1769–1777. <https://doi.org/10.1021/acsomega.7b00103>.
- (16) Walther, F.; Davydovskaya, P.; Zürcher, S.; Kaiser, M.; Herberg, H.; Gigler, A. M.; Stark, R. W. Stability of the Hydrophilic Behavior of Oxygen Plasma Activated SU-8. *J. Micromech. Microeng.* **2007**, *17* (3), 524. <https://doi.org/10.1088/0960-1317/17/3/015>.
- (17) Wang, Y.; Bachman, M.; Sims, C. E.; Li, G. P.; Allbritton, N. L. Simple Photografting Method to Chemically Modify and Micropattern the Surface of SU-8 Photoresist. *Langmuir* **2006**, *22* (6), 2719–2725. <https://doi.org/10.1021/la053188e>.